

THE DEVELOPMENT OF 3D SUB-SURFACE MAPPING SCHEME AND ITS APPLICATION TO MARTIAN LOBATE DEBRIS APRONS

Hyunseob Baik^a, Jungrack Kim^{b*}

^a Dept. of Geophysical Exploration, KIGAM school of University of Science and Technology, Daejeon, Korea -
hsbaik@kigam.re.kr

^b Dept. of Geoinformatics, University of Seoul, Seoul, Korea - kjrr001@gmail.com

Commission III, ICWG III/II

KEY WORDS: SHARAD, Topographic data, Subsurface mapping, LDA, Mars

ABSTRACT:

The Shallow Subsurface Radar (SHARAD), a sounding radar equipped on the Mars Reconnaissance Orbiter (MRO), has produced highly valuable information about the Martian subsurface. In particular, the complicated substructures of Mars such as polar deposit, pedestal crater and the other geomorphic features involving possible subsurface ice body has been successfully investigated by SHARAD. In this study, we established a 3D subsurface mapping strategy employing the multiple SHARAD profiles. A number of interpretation components of SHARAD signals were integrated into a subsurface mapping scheme using radargram information and topographic data, then applied over a few mid latitude Lobate Debris Aprons (LDAs). From the identified subsurface layers of LDA, and the GIS data base incorporating the other interpretation outcomes, we are expecting to trace the origin of LDAs. Also, the subsurface mapping scheme developed in this study will be further applied to other interesting Martian geological features such as inter crater structures, aeolian deposits and fluvial sediments. To achieve higher precision sub-surface mapping, the clutter simulation employing the high resolution topographic data and the upgraded clustering algorithms assuming multiple sub-surface layers will be also developed.

1. INTRODUCTION

In terms of paleo climatic conditions which could create habitable environment, the subsurface structure of Martian topography has been largely interested by science community. It's because the footprints of some crucial environmental factors such as precipitation, glaciation and permafrost may remain in the underground layers of Mars. Therefore, Ground Penetration Radar (GPR), for instance the Mars Advanced Radar for Subsurface and Ionosphere Sounding (MARSIS) on the Mars Express and Shallow Subsurface Radar (SHARAD) on the Mars Reconnaissance Orbiter (MRO) employing very long electromagnetic wave and its high penetration depth has been actively introduced. The challenges of mining underground information with GPR are 1) the minimization of a various noise components such as ionospheric interferences and signal delay; 2) the conversion of time domain reflectance from underground layers into the high dimensional (2D/3D) mapping products for the better interpretation; 3) effective tracing discontinuities from subsurface layers especially compared to clutter simulation. Thus, we tried to develop a preliminary surface mapping scheme integrating all the technical components to address the aforementioned problems and applied to a certain geomorphological target, i.e. Lobate Debris Aprons (LDA).

First, all SHARAD profiles over a target geomorphological feature were collected along with the clutter simulation employing Mars Orbiter Laser Altimeter (MOLA) Digital Terrain Model (DTM). To more clearly identify the subsurface discontinuities in SHARAD profiles, we introduced noise filtering based on radon transformation. After then, the interpretation of 3D SHARAD profiles and their clutter simulations allowed identifying the trails of sub-surface layers. Considering the error range in dialectic coefficients of potential

subsurface layers, a clustering algorithm was developed and iteratively applied together with the gridding procedure to organise the optimal 3D planes of sub-surface signal discontinuities. After all, the outcomes extracted from our test target areas over Euripus Mons and Promethei Terra LDAs were demonstrated and analysed with the involved geological contexts.

2. BACKGROUND

2.1 Sensor

The idea to use highly low frequency domain radar sounder, so called space borne GRP, for the mapping of the upper portions Martian crust was firstly introduced by MARSIS equipped in Mars Express (Picardi et al., 2004). Although, the demands to investigate distribution of liquid and solid water as the footprint of Martian geological evaluation had been actively proposed as shown in Carr (1996), the main focus of MARSIS observation was on the Martian polar deposits which are obviously significant ice (or dry ice) objects in solar systems and have crucial acting roles in the atmospheric circulation and the evolution (Picardi et al., 2005; Zuber et al., 2007) of Mars. Shortly thereafter, the capabilities of MARSIS were complemented by SHARAD of MRO with the better vertical resolution but a lower penetration capability compared to MARSIS. SHARAD was developed by Italian Space Agency and Jet Propulsion Laboratory and launched in 2005. It has 20 MHz centre frequency, 10 MHz bandwidth and 15m free space horizontal resolution (Seu et al., 2007). SHARAD has been successfully used to observe complicate substructures of Mars, not only polar deposit but also the other geomorphic features involving possible subsurface ice body even including rather small scale objects such as pedestal craters (Nunes et al., 2001)

* Corresponding author.

and LDAs (Holt et al., 2008). Therefore, considering its better potential to extract the information on surface layering, we focused our analysis on data gathered with SHARAD rather than MARSIS though the efforts to further exploit MARSIS data are still undergoing.

2.2 Introduction of Target object

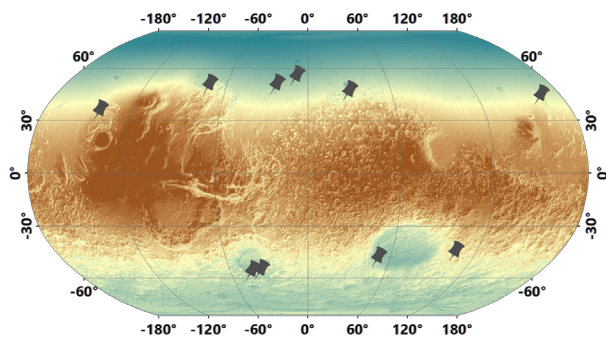


Figure 1. Martian-wide distribution of LDAs.

LDA, which is the target object of this study, is regarded as an evidence of potential glacial process (Holt et al., 2008) and ice debris transport in ancient Martian environment (Hauber et al., 2008). It can be characterized as alluvial-fan-like debris with tens to hundreds meters thick mass flowed from the mountain slope that was covered by glacier or periglacial landforms around some Million Years ago, estimated by crater counting (van Gasselt et al., 2016). Although, geomorphic and physical interpretations of LDA are actively undergoing, its detailed origin remains unclear. Accordingly, subsurface mapping of LDAs employing radargram analysis and SHARAD data could be useful for identifying clues about the origins of those geomorphic structures.

LDAs are most intensively distributed in mid-latitude regions (see Figure 1) along with the dichotomy of the northern hemisphere and southern megabasins (van Gasselt., 2007). Since those highland features were presumably covered with glacier and certain sediments in Amazonian age, it was regarded as an evidence of paleo-glacial activity at Mars. Then it was proposed that climate change with a certain reason induced the melting of the Martian glaciers and sediments that covered the glacier slid down through the steep side and produced the present fan-shaped LDA (see Figure 2).

In this study, considering their geomorphic characteristics, two sites, i.e., Euripus Mons and Promethei Terra LDAs (44.8S 105.2E) were chosen for the target of SHARAD subsurface mapping. Recently, relatively high ice content over underlying has been already identified (Holt et al., 2008) in those target areas and proposed that at least some of them might be composed of pure ice, protected from sublimation by a thin debris cover. A modelling work assuming glacial deformation helped to reconstruct some internal structural properties (Karlsson et al., 2015). Despite these attempts, Euripus Mons shows clear geomorphic signatures of classical periglacial denudation which do not fit into the concept of glacial-only evolution (van Gasselt et al., 2016; Kim et al., 2016). Therefore, over these target areas, we tried to identify subsurface structures which may imply important clues about the origin of LDA and its deposits, employing SHARAD track profiling.

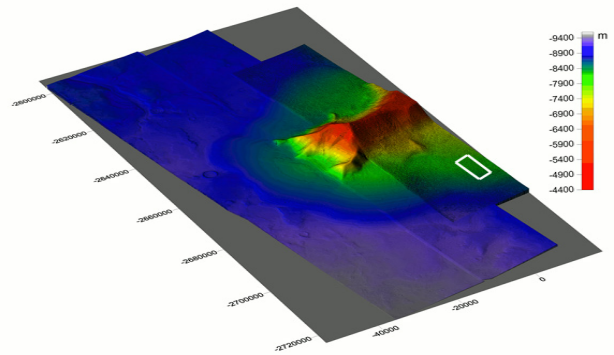


Figure 2. CTX DTM mosaic over Euripus Mons (sinusoidal projection, center of longitude=105°E) Stereo processing scheme were stated in Kim and Muller (2009) and Kim et al. (2016)

3. METHODS

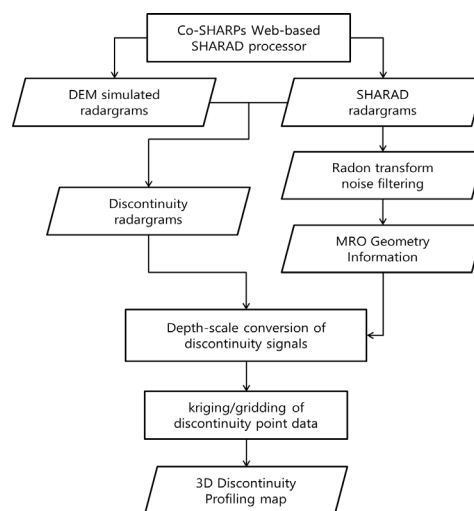


Figure 3. Flow chart of this study.

The purpose of SHARAD processing in this study is to discriminate subsurface layer using clearly identified discontinuities and their 2D/3D distributions. The outline of processing chain was shown in Figure 3 and the sub-steps of established process are as follows.

1. Identification of SHARAD tracks (Figure 4) and collection of SHARAD Reduced Data Records (RDR) data from NASA's Orbital Data Explorer (ODE)
2. Radargram processing by Co-SHARPs Processing Boutique (Putzig et al, 2016) and clutter simulation using MOLA DTM.
3. Radargram noise reduction preprocess by Radon transformation (Figure 5).
4. Subsurface discontinuity extraction (Figure 6) from clutter simulation and SHARAD radargram.
5. Depth conversion using the relationship

$$d = [c/\sqrt{\epsilon}] * t / 2 \quad (1)$$

where d = the depth, c = speed of light, ϵ = dielectric permittivity and t = delay time of signal.

6. Discontinuity clustering considering estimated depth error and spatial proximity.
7. Co-kriging and iterative refinements of clustered subsurface discontinuities.

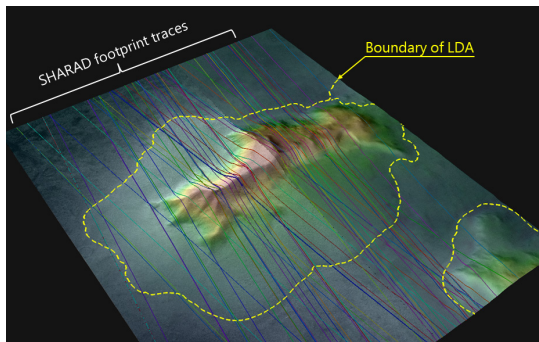


Figure 4. HRSC DTM mosaic over Euripus Mons LDA and overlaid SHARAD tracks.

3.1 Pre-processing

The SHARAD radargram exhibits a considerable amount of speckles that complicates analyses of small structures. To overcome speckles issue, we conducted a radargram noise reduction process to detect clear subsurface discontinuity with radon transformation and noise filtering techniques. First proposed in the early 20th century, the radon (τ - p) transformation, which can reconstruct the shape and characteristics of the original object from projected data from various directions, has become an efficient tool for migrating the error of GPR data (Pasolli et al., 2009; Wang and Oristaglio, 2000), especially for linear structure analysis. Since the mentioned advantages of radon transformation accommodated our objective of subsurface layer detection, we projected the original radargram to radon (τ - p) domain and filtered signals in a -10 – 10 -degree range in the τ - p domain (Figure 5). After noise filtering, we applied a high-pass filter with 3×3 kernel to extract the clear radar signal.

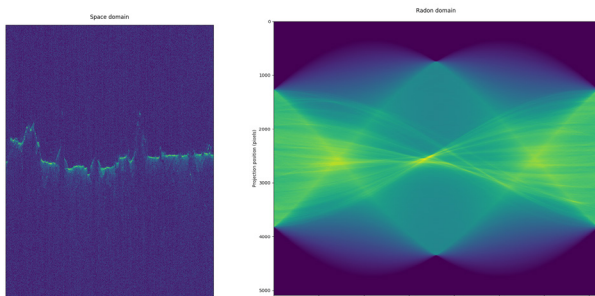


Figure 5. Radon transformation of radargram. Left: original radargram (track 0876801). Right: Radon transformation result.

3.2 Discontinuity extraction

After preprocessing, we produced clutter simulation data by using the Co-SHARPs Processing Boutique (Putzig et al., 2016), a web-based SHARAD and DTM clutter simulation server with remote access. Thus, over all tracks in target areas, we conducted clutter simulations based on MOLA DTM and compared them with SHARAD radargrams in order to identify subsurface discontinuities (Figure 6). Accordingly, we processed 50–70 radargrams at each target area and pinpointed all discontinuities.

We performed the 3D rearrangement of the discontinuity points by using the footprint geometry file of SHARAD radargrams. With the MRO pointing geometry and digital elevation model of Mars, georeferencing the SHARAD radargram and clutter simulation was feasible. Ultimately, we achieved projections of

surface discontinuity into 3D coordinates as represented in Figure 7.

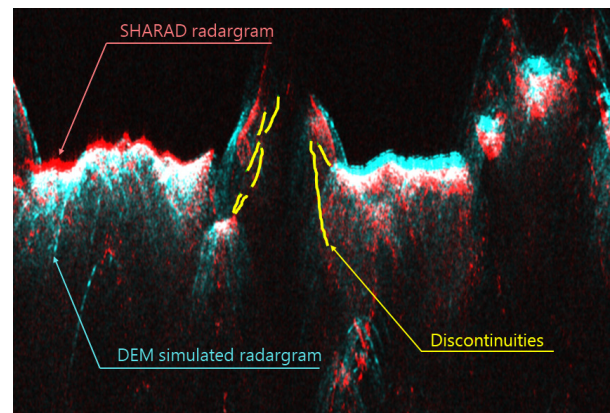


Figure 6. Discontinuity detection by the Intercomparing between SHARAD radargram (red) and clutter simulation (right). Subsurface discontinuities (yellow) are extracted from the observations of difference between profiles.

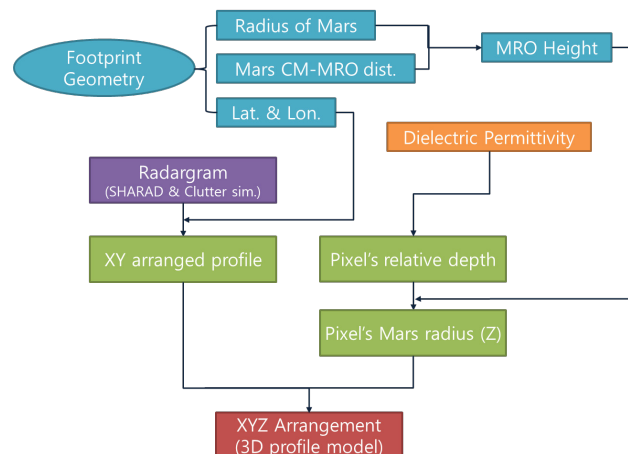


Figure 7. Discontinuity detection from comparing SHARAD radargram (red) and clutter simulation (right). Subsurface discontinuities (yellow) are extracted from the difference between two radargrams.

3.3 Discontinuity Point classification

After collecting all discontinuities of sublayers, the points were classified visually into a few initial groups according to their spatial distributions. Co-kriging was applied to extract interpolated sublayer planes and then the Euclidian distances between discontinuity points and the interpolated planes were calculated. By an iterative procedure to attain optimal number of clusters and distances, the best fit underground sublayers were extracted. At the moment, we are employing manual interaction to accomplish this task; however the automated/semi-automated routine is under development.

4. RESULTS

4.1 Pre-processing

In the preprocessing stage consisting of radon transformation and filtering, noise speckles in radargrams decreases dramatically. As shown in Figure 8, the radargram processed by the radon transformation and noise filtering showed far clearer

backscattering signal, and its white noise component improved considerably. Consequently, the subsurface layers of the LDA of Promethei Terra showed better details than with the unfiltered radargram (Figure 9).

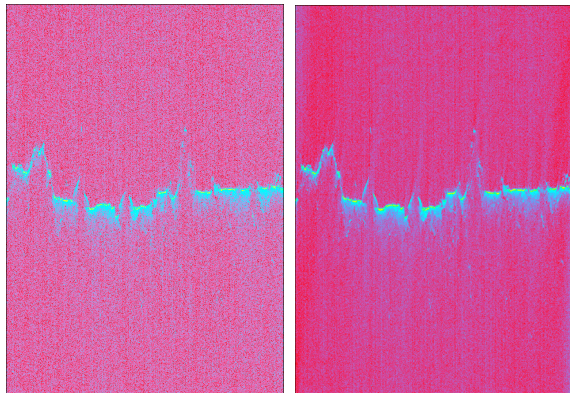


Figure 8. Original radargram (left) and Radon transformation noise-filtered radargram (right). Note a significant improvement in backscattering quality

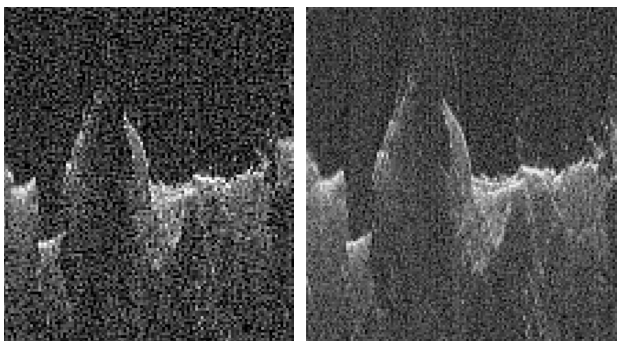


Figure 9. A noise filtering result in magnified radargram over Promethei Terra LDA. Original radargram (left) and noise-filtered radargram after radon filtering (right)

4.2 3D subsurface mapping

After a sequence of procedures involving preprocessing, discontinuity detection, and point classification, we clearly identified the gridded subsurface structures of the LDAs of Euripus Mons and Promethei Terra. We discovered three discontinuity sublayers underneath the LDA of Euripus Mons, represented with red, green, and blue in Figure 10. Interestingly, the morphologies of surface layers differ considerably in northern and southern aprons, which implies the effects of illumination conditions in the geomorphic evolution. Over Promethei Terra, we identified two layers (Figure 11) and also different morphologies in the northern and southern aprons. On the other hands, our subsurface 3D mapping results demonstrated significant vertical displacements between the layers. The sublayers exist at depths of 500, 1,200 and 1,800 m from the topography of the LDA of Euripus Mons and at depths of 400 and 600 m at the LDA of Promethei Terra (Figure 10 and 11). We propose that such unsymmetrical shapes and relatively large depths of subsurface layers imply important clues about the morphological evolutions of LDAs.

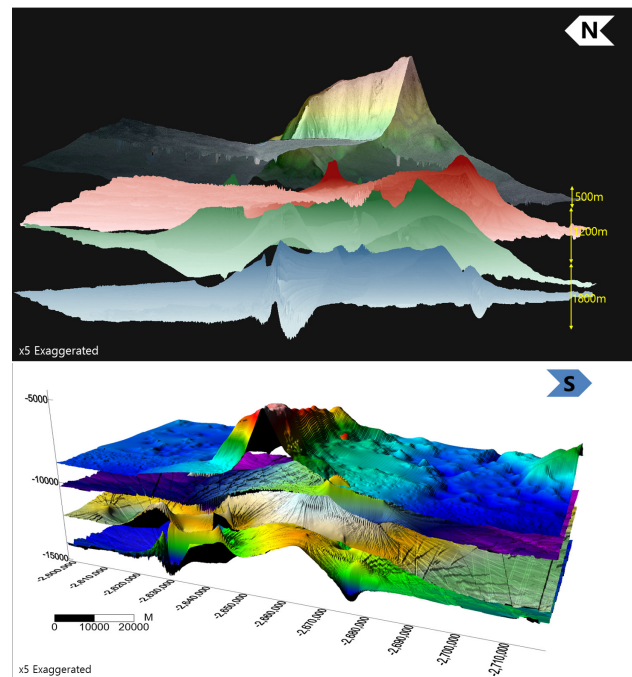


Figure 10. Euripus Mons LDA's subsurface mapping result. Note topographies over target areas are represented by HRSC orthorectified image and HRSC & MOLA DEM.

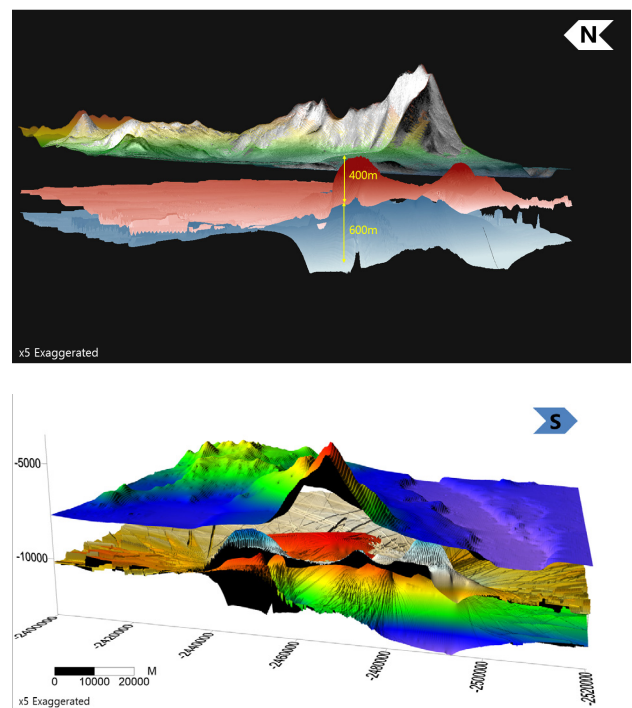


Figure 11. Promethei Terra LDA's subsurface mapping results.

5. CONCLUSIONS

Although analyses of data collected with GPR such as MARSIS and SHARAD offer a large amount of interesting clues about Martian surface and climate evaluations, their interpretations continue to depend upon the 1D profiling of signals. Therefore, we developed a 3D subsurface mapping procedure that can facilitate the definition of subsurface layers from SHARAD signals by employing a filtering scheme involving radon transformation, discontinuity detection involving radar signal

analyses, and point classification together with spatial interpolation. Upon applying the procedure over LDAs in Euripus Mons and Promethei Terra, we identified multiple subsurface layers. Given our previous stereo processing results (Kim et al., 2016), which clearly show scalloped depressions over aprons, we inferred that the layers had originated during periodic sublimation events, which imply occasionally thick mass debris flows and periodic climate changes. We are planning the improvements of the established algorithms as follows; 1) introduction of High Resolution Stereo Camera (HRSC) and Context Camera (CTX) stereo DTMs for clutter simulations; 2) semi-automated sub-surface layering employing Support Vector Machine (SVM) algorithms. Accordingly, we should be able to more clearly investigate the origin of LDAs by using the applications of the new subsurface mapping procedure. Ultimately, our method could also be applied to study a great deal of Martian geomorphologies.

REFERENCES

- Carr, M.H. 1996. *Water on Mars*, Oxford University Press, Oxford, UK
- Hauber, E., S. van Gasselt, M. G. Chapman, and G. Neukum 2008. Geomorphic evidence for former lobate debris aprons at low latitudes on Mars: Indicators of the Martian paleoclimate, *Journal of Geophysical Research: Planets*, 113, E02007, doi:10.1029/2007JE002897.
- Holt, J. W., Safaeinili, A., Plaut, J. J., Head, J. W., Phillips, R. J., Seu, R., ... & Biccari, D. 2008. Radar sounding evidence for buried glaciers in the southern mid-latitudes of Mars. *Science*, 322(5905), 1235-1238.
- Karlsson, N. B., Schmidt, L. S., & Hvidberg, C. S. 2015. Volume of Martian midlatitude glaciers from radar observations and ice flow modeling. *Geophysical Research Letters*, 42(8), 2627-2633.
- Kim, J. R., Baik, H., van Gasselt, S. 2016. Constraints on Landscape Formation of Euripus Mons, Mars, from Topographic and Radar Data Analysis. *Sixth international Conference on Mars Polar Science and Exploration*, September 5-9, 2016 in Reykjavik, Iceland.
- Kim, J. R., & Muller, J. P., 2009. Multi-resolution topographic data extraction from Martian stereo imagery. *Planetary and Space Science*, 57(14), 2095-2112.
- Nunes, D. C., Smrekar, S. E., Fisher, B., Plaut, J. J., Holt, J. W., Head, J. W., ... & Phillips, R. J. 2011. Shallow Radar (SHARAD), pedestal craters, and the lost Martian layers: Initial assessments. *Journal of Geophysical Research: Planets*, 116(E4).
- Pasolli, E., Melgani, F., & Donelli, M. 2009. Automatic analysis of GPR images: A pattern-recognition approach. *IEEE Transactions on Geoscience and Remote Sensing*, 47(7), 2206-2217.
- Picardi, G., Biccari, D., Seu, R., Plaut, J., Johnson, W. T. K., Jordan, R. L., ... & Bombaci, O. 2004. MARSIS: Mars Advanced Radar for Subsurface and Ionosphere Sounding. *MARS EXPRESS*, 51.
- Picardi, G., Plaut, J. J., Biccari, D., Bombaci, O., Calabrese, D., Cartacci, M., ... & Federico, C. 2005. Radar soundings of the subsurface of Mars. *Science*, 310(5756), 1925-1928.
- Putzig, N. E., Phillips, R. J., Campbell, B. A., Plaut, J. J., Holt, J. W., Bernardini, F., ... & Smith, I. B. 2016. Custom SHARAD Processing via the CO-SHARPS Processing Boutique. *47th Lunar and Planetary Science Conference, Houston, Tx, USA* (Vol. 47, p. 3010).
- van Gasselt, S. 2007. Cold-climate landforms on Mars. Dissertation. Freie Universität Berlin, Germany.
- van Gasselt S., Kim J.-R., Baik H. 2016. Landform Evolution and Climate Constraints in Promethei Terra. *European Geosciences Union General Assembly 2016*. Vienna, Austria
- Wang, T., & Oristaglio, M. L. 2000. GPR imaging using the generalized Radon transform. *Geophysics*, 65(5), 1553-1559.
- Zuber, M. T., Phillips, R. J., Andrews-Hanna, J. C., Asmar, S. W., Konopliv, A. S., Lemoine, F. G., ... & Smrekar, S. E. 2007. Density of Mars' south polar layered deposits. *Science*, 317(5845), 1718-1719.